



## The Behavior of Itakpe Iron-Ore Tailings in One-dimensional Compression

*T. D. Olaiya<sup>1\*</sup>, B. O. Taiwo<sup>1</sup>*

<sup>1</sup>The Federal University of Technology, Akure, Nigeria

Corresponding author email: [olaiyamne168188@futa.edu.ng](mailto:olaiyamne168188@futa.edu.ng)

### ABSTRACT

Tailing dam failure can be so hazardous and result in irrevocable environmental impacts. In recent years, more attention has been paid to the mechanical behavior of tailing geo-materials by the geomechanics in an attempt to understand better their behavior so that safe tailing dams can be constructed. This study investigates the behavior of iron ore tailings obtained from Itakpe, Kogi State, Nigeria, in an incremental oedometer loading. The samples were prepared by different methods and discussions were made as regards effects of sample preparation and the possibility of any transitional behavior in the samples. Comparisons are made between the present iron ore tailings and previously published data on iron ore tailings and other geo-materials. The compression curves do not converge to a unique line and this is an indication of a normal compression line. The methods of sample preparation have a very negligible effect on the compression behavior of the materials.

Keywords: Tailings, Iron-ore, Oedometer, Compression behavior, Geo-materials

### 1. Introduction

Iron ore is a name used to refer to rocks that contain sufficient amount of iron that is applicable in different industries and it comprises of varieties of minerals ranging from hematite ( $\text{Fe}_2\text{O}_3$ ), magnetite ( $\text{Fe}_3\text{O}_4$ ), siderite ( $\text{FeCO}_3$ ) and limonite ( $\text{FeO}(\text{OH}) \cdot n(\text{H}_2\text{O})$ ) (Wells et al., 2014). Iron accounts for closely 95% of all metals used by industries of this age and almost 98% of the iron ore content is used in the production of steel (Marshall and Robert, 2014). Iron ore is being beneficiated all around the world to meet the raw materials requirements of the iron and steel industries. Due to the high industrial demand on steel, the extraction of iron ore becomes very pertinent by different mining industries. The exploitation and concentration process of iron ore produces large quantity of waste materials called tailings. According to Franks et al (2011) tailings as by-products of concentrated minerals or the left-over materials after economic minerals have been successfully recovered from the uneconomic fractions of an ore. Tailings consist of fine particles of crushed ore, high quantity of water, traces of metals and chemicals used in the concentration process. Chao et al (2019) indicated that the high-water content and small grain sizes of the tailings when disposed make its mechanical strength and stability to be very poor. The disposal and storage of tailings becomes a significant concern for the entire extraction and processing operation. There is an urgent need to enhance safety in design and operation of tailing dams which is solely dependent on the mechanical behavior of tailings used for construction of the dam as well as geology of disposal site.

Christian and Baecher (2001) noted that the Strength analysis provides a frame work for establishing appropriate factors of safety and other design targets and leads to a better appreciation of the relative importance of uncertainties in different parameters. Strength analysis can be used to assess the suitability of iron ore tailing in its industrial application. Many studies have been conducted to investigate the compression behavior of mine tailings and the results differs with different kinds of tailings analyzed (Wong *et al.*, 2008; James *et al.*, 2011; Geremew and Yanful, 2013; Bonin *et al.*, 2014). Providing a comprehensive understanding of mechanical properties of mine tailing is very crucial for the design of tailing dams and identification of its industrial applications. This project examines a one-dimensional compression behavior of iron tailings.

#### 1.1 Description of the study area

The study area is located at Okehi Local Government, Itakpe, Kogi State, Nigeria. The deposit is mainly composed of magnetite and hematite minerals and consist of 14 layers of ore which are economically valuable. The percentage of iron ranges in grade from 14.8% to 41% with an overall grade of 36%. It has an estimated reserve of 182.5 million metric tons consisting mainly quartz, magnetite and hematite (Nwosu *et al.*, 2013). The mine face at this company is divided into eastern and western part with operation starting from the western face at 320m above mean sea level and stripping ratio of 1:4. The deposit is located at latitude  $07^{\circ} 36' 20''$  N and  $06^{\circ} 18' 35''$  E. location map for the study area is shown in figure 1 below.

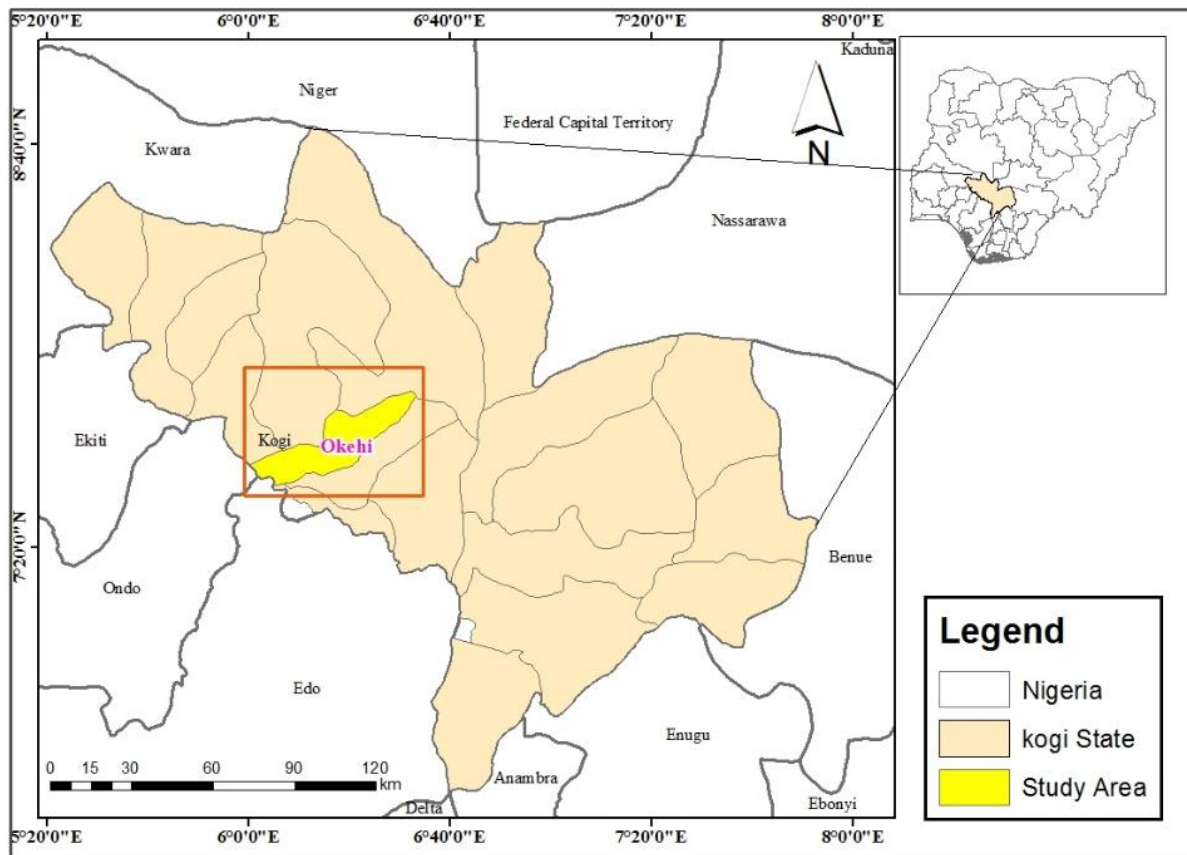


Fig. 1Map showing the Study Area

## 2.Methods and Test Procedures

The samples used are iron ore tailing materials and they are referred to as reconstituted materials because their grain sizes are not evenly distributed and the bond holding the grains together has been altered. These samples were collected in loosed form at different depths (top and base) and prepared in dry, wet and slurry condition and then subjected to six different tests to study their behavior under incremental loads. Okewale, (2020) noted that investigation of samples is better done at different depths due to redistribution of grain sizes and likely variability in water content as the depth increases. For the odometer consolidation, the weights 0.1 kg, 0.2 kg, 0.5 kg, 1 kg, 2 kg, 5 kg, 10 kg, 20 kg, 40 kg and 56 kg were added respectively at specified time interval were used to compress the sample under test. Three different sample preparation methods were adopted for the compression test; dry compression, wet compression, and slurry, to investigate whether this would affect the behavior of the samples. For the dry compaction method, the tailings were oven dried and then sprinkled gently into the oedometer ring from a constant height to achieve loose samples. A steel rod was used to compact the tailings with different number of impacts to ensure that the sample was appropriately fixed inside the ring.

Generally, the samples were divided into three layers, and the first layer was compacted with less effort using the steel rod and the upper layer with greater effort to achieve a more uniform density of the sample along its longitudinal axis. Wet samples were prepared by adding varying quantities of distilled water to the samples. Although, not to any targeted initial density or water content (Okewale and Coop 2017). The reconstituted samples were placed and mixed in sample container. For the slurry method, distilled water was gradually added into the dry tailings until the water content was close to or a little higher than the liquid limit.

It is of importance to note that different acronyms shall be used to denote the sample preparations in subsequent pages. For instance, TD1 and BD1 will represent the top-dry samples 1 and Base-dry samples 1 respectively with the first letter representing the sample location as regards depth (T = Top, B = Base) and the last letter representing the nature of sample as regards water content.

Considerable quantity of sample was put in a predetermined weight of container and measured using electric weighing balance. The sample was then placed in an oven for 24 hours to allow complete disappearance of its moisture content. The weight of sample together with the container was measured after oven drying. The initial water content ( $W_i$ ) of the sample was recorded as weight of container with sample before drying minus the weight after drying.

$W_i$  = weight of (can + sample) before drying - weight of (can + sample) after drying.

A measured quantity of sample was placed in the oedometer ring and the weight recorded as the initial weight of loaded sample ( $M_i$ ). The sample was later covered with a loading cap of about 105 g. When preparing the sample, filter papers were added between the tailings and the confining ring to avoid interference of unnecessary moisture and clogging of sample on the ring. Water was added into the reservoir around the sample, so the sample

remains saturated during test. The sample was then mounted in the consolidation cell and the initial reading was taken before any addition of load. Weights of 0.1 kg, 0.2 kg, 0.5 kg, 1 kg, 2 kg, 5 kg, 10 kg, 20 kg, 40 kg and 56 kg were added respectively, each at a specified time interval (30 minutes precisely) before the other and the dial gauge readings were recorded accordingly. The sample was unloaded to 20 kg, 5 kg and 0.5 kg respectively and the dial gauge readings were also recorded.

After unloading, the sample was dismantled, re-weighed and oven-dried to observe the level at which it has absorbed water. The final weight of sample ( $M_f$ ) and the final water content ( $W_f$ ) were recorded.  $W_f$  = weight of (can + sample) after loading - weight of (can + sample) after drying.

## 2.1 Behavior of Geomaterials

The behavior of geomaterials in one-dimensional compression was studied by employing conventional front loading oedometer. In order to describe the behavior of the geomaterials, specific volume,  $v$  ( $v = 1+e$ , where “e” is the void ratio) is considered to be very important along with stress,  $\sigma$  (kpa) as indicated by Okewale (2020b; Okewale and Grobler 2020a). Okewale (2020b) indicated that the specific volumes can be determined using different methods to improve the confidence in the measurements with the initial specific volumes of the sample determined from sample weight, initial height, diameter and water content.

The final specific volume was estimated from final weight and dimensions. Adopting the back-calculating approach (Equation 1-4), the initial value was used with the vertical strain measured in the tests (Okewale and Coop 2017; Okewale, 2020b). The vertical strain is obtained by dividing the overall settlement by the average initial height. Four different equations have been used for determination of specific volume and the equations were made to be as independent as possible (Okewale, 2020b).

$$V_i = W_i G_s + 1 \quad (1)$$

$$V_i = \frac{\gamma_w (1+W_i) G_s}{\gamma_{bi}} \quad (2)$$

$$V_i = \frac{\gamma_w (1+W_f) G_s}{\gamma_{bf} (1-\varepsilon_v)} \quad (3)$$

$$V_i = \frac{W_f G_s + 1}{(1-\varepsilon_v)} \quad (4)$$

Where:  $W_f$  is the final water content  $\gamma_w$  is the unit weight of water  $\gamma_{bi}$  is the initial bulk unit weight  $\gamma_{bf}$  is the final bulk unit weight  $\varepsilon_v$  is the vertical strain  $V_i$  is the initial specific volume  $G_s$  is the specific gravity  $W_i$  is the initial water content.

The specific volume is an intrinsic property of a material which defines the number of cubic meters occupied by one kilogram of a particular substance in the material.

Specific volume is expressed in material science as 1 plus void ratio (e) of the material. Specific volume,  $v = 1 + e$ .

The specific gravity ( $G_s$ ) of a soil refers to the ratio of the solid particles' unit weight to the unit weight of water. It is also used to derive several important soil parameters such as the porosity, dry and saturated density and the degree of saturation. The specific gravity ( $G_s$ ) of iron ore tailings was measured following ASTM (2002a) standard, giving the value of 2.99 The initial water content of the test is measured before application of loads. It is expressed as weight of sample with the container before drying minus the weight after oven-drying.

The final water content of the test is measured after application of loads. It is expressed as weight of sample with the container before drying minus the weight after oven-drying.

Initial bulk unit weight of the material is measured before applying loads. It is calculated as initial mass of the material divided by the volume while the final bulk unit weight of the material is measured after applying loads. It is calculated as final mass of the material divided by the volume. The initial and final bulk unit weight was calculated by Equations 5 and 6 below.

$$\gamma_{bi} = \frac{M_i}{\pi \times \left[\frac{d}{2}\right]^2 \times h_i} \quad (5)$$

$$\gamma_{bf} = \frac{M_f}{\pi \times \left[\frac{d}{2}\right]^2 \times h_f} \quad (6)$$

Where:  $M_i$  is the weight of sample before loading,  $M_f$  is the weight of sample after loading,  $h_i$  is the initial height of sample in the ring before loading,  $h_f$  is the final height of sample in the ring after loading and  $d$  is the diameter of the ring.

### 3. Results and Discussion

Figure 2-4 presents the compression behavior of Top-dry (TD) samples, Top-Wet (TW) samples, and Top-Slurry (TS) samples respectively. Table1 presents the result of the oedometer tests for the samples.

Table1: Summary of One-dimensional Compression Test

Sample Location	Preparation Methods	Test Number	$\phi$ (mm)	$w_i$ (%)	$w_f$ (%)	$v_i$	$v_f$	$\sigma v(\max)$ kpa	Acc. ( $\pm$ )
TOP	DRY (TD)	1	30	3.8	15.9	1.5552	1.5399	8542	0.06
		2	30	3.2	15.8	1.5888	1.5704	8542	0.03
		3	30	4.4	14.9	1.5789	1.3218	8542	0.09
		4	30	5.6	15.2	1.5522	1.4928	8542	0.01
		5	30	4.3	12.7	1.5247	1.3530	8542	0.04
		6	30	3.1	15.4	1.5770	1.3312	8542	0.06
	WET (TW)	1	30	7.0	16.01	1.6774	1.5988	8542	0.01
		2	30	7.3	17.3	1.6765	1.6320	8542	0.07
		3	30	7.1	18.2	1.5303	1.4264	8542	0.06
		4	30	6.8	10.8	1.6543	1.6305	8542	0.007
		5	30	4.6	15.8	1.5567	1.5204	8542	0.002
		6	30	5.6	15.1	1.9365	1.8925	8542	0.09
	SLURRY (TS)	1	30	22.7	17.1	1.5665	1.4852	8542	0.08
		2	30	24.2	17.1	1.6216	1.5176	8542	0.01
		3	30	26.1	16.1	1.5798	1.3312	8542	0.005
		4	30	25.4	18.8	1.7562	1.6613	8542	0.004
		5	30	23.7	17.2	1.7351	1.6846	8542	0.02
		6	30	26.6	16.8	1.7804	1.7282	8542	0.01
BASE	DRY (BD)	1	30	5.9	18.3	1.5626	1.5219	8542	0.03
		2	30	7.3	18.9	1.6778	1.6327	8542	0.06
		3	30	6.6	16.7	1.5909	1.5241	8542	0.01
		4	30	5.2	16.7	1.7400	1.6619	8542	0.01
		5	30	4.1	22	1.6904	1.6618	8542	0.09
		6	30	3.9	19	1.6310	1.6024	8542	0.08
	WET (BW)	1	30	7.9	21	1.6902	1.5889	8542	0.05
		2	30	7.3	12.7	1.6657	1.6251	8542	0.03
		3	30	6.9	10.7	1.8868	1.4557	8542	0.004
		4	30	6.8	13.4	1.6487	1.6111	8542	0.08
		5	30	7.5	19.8	1.4230	1.2995	8542	0.01
		6	30	6.8	10.7	1.6228	1.3868	8542	0.04
	SLURRY (BS)	1	30	15.8	18.4	1.6448	1.5862	8542	0.04
		2	30	30.2	19.2	1.8769	1.7331	8542	0.02
		3	30	18.5	10.1	1.4049	1.2096	8542	0.01
		4	30	33.8	26.8	2.0704	1.5745	8542	0.05
		5	30	24.2	18.8	1.6681	1.4828	8542	0.05
		6	30	21.6	15.3	1.7145	1.5651	8542	0.09

NOTE:  $\phi$  is diameter of sample (mm);  $w_i$  &  $w_f$  are initial and final water content (%) respectively,  $v_i$  &  $v_f$  are the initial & final specific volume respectively,  $\sigma v(\max)$  is the vertical effective stress, and acc. ( $\pm$ ) is the accuracy of specific volume.

Figure 2 present the result of the One-dimensional compression behavior for the top dry (TD) samples. The compression behavior of reconstituted sample is termed intrinsic or inherent behavior as indicated in Okewale,(2020b) work. This behavior is solely dependent on the constituent particles of the soil and it is very essential because inherent compressibility parameters of geomaterials are required for engineering design. The compression curves of the TD samples show a very slow convergence at a vertical effective stress of about 8 MPa.

Figure 3 shows one dimensional compression behavior of samples TW. It reveals that the compression curves from different initial densities give a relatively slow convergence.

As represented in the Figure 4, it was revealed that the slurry samples show a non-convergent behavior at a maximum vertical effective stress of 8 MPa and the unique normal compression line cannot be identified. Different sample preparation methods for the top samples show almost the same convergence, so it can be considered that the preparation methods adopted for the top samples does not significantly affect the sample behavior.

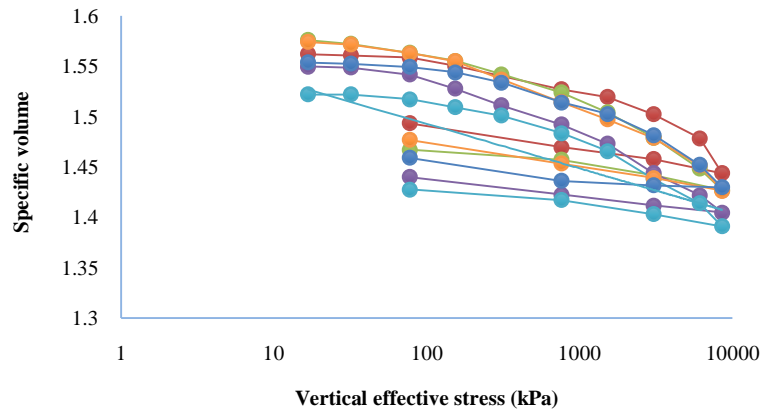


Figure 2: Compression Behavior of Samples TD.

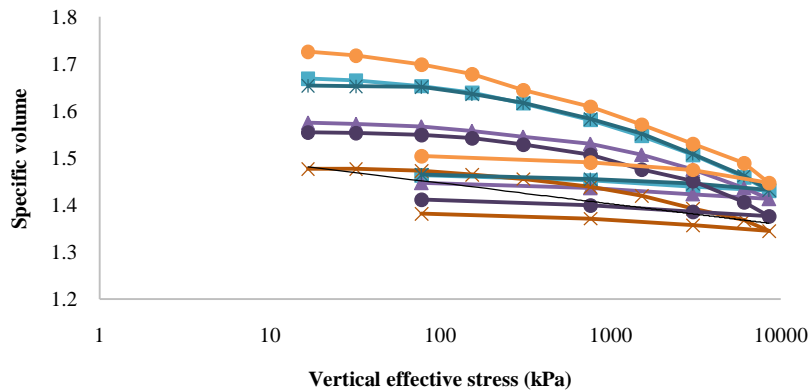


Figure 3: Compression Behavior of Samples TW

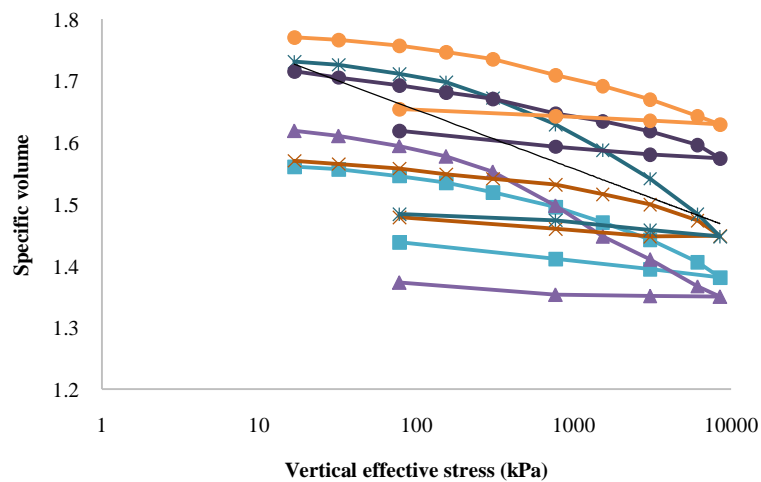


Figure 4: Compression Behavior of Samples TS

Figure 5-7 present the compression curves which are fairly similar and the paths do not converge to unique normal compression lines. Such behavior is termed intrinsic behavior and it has been reported in Ire Ekiti tropical clay (Okewale and Grobler, 2021).

Figure 5 represents one-dimensional compression behavior for the samples BD. Similar to the top samples, the compression curves of the dry samples show a very slow convergence and the unique one-dimensional normal compression line (1D-NCL) cannot be obtained after reaching a maximum vertical effective stress of about 8 Mpa.

Figure 6 represents one-dimensional compression behavior for the samples BW. This is also very similar to the wet samples obtained from the surface (top), the compression curves show a much slower convergence and the unique one-dimensional normal compression line (1D-NCL) cannot be obtained after reaching a maximum vertical effective stress of about 8 Mpa. It can be considered that samples which were prepared in the same way have almost the same compression behavior.

The slurry samples show a much apparent non-convergence behavior as represented in the Figure 7. This is very much similar to the slurry samples

from the top even though they were obtained at relatively different depths. It can then be considered that the compression behavior for the slurry samples is not affected by depths at which the samples were obtained.

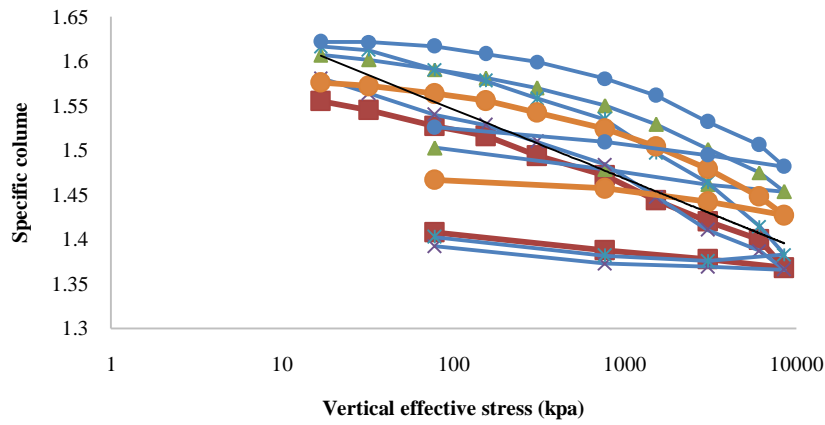


Figure 5: Compression Behavior of Samples BD

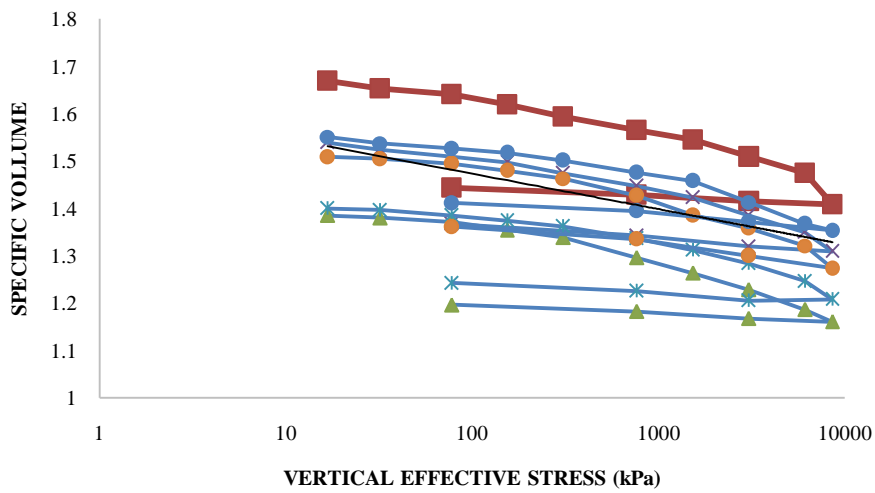


Figure 6: Compression Behavior of sample BW

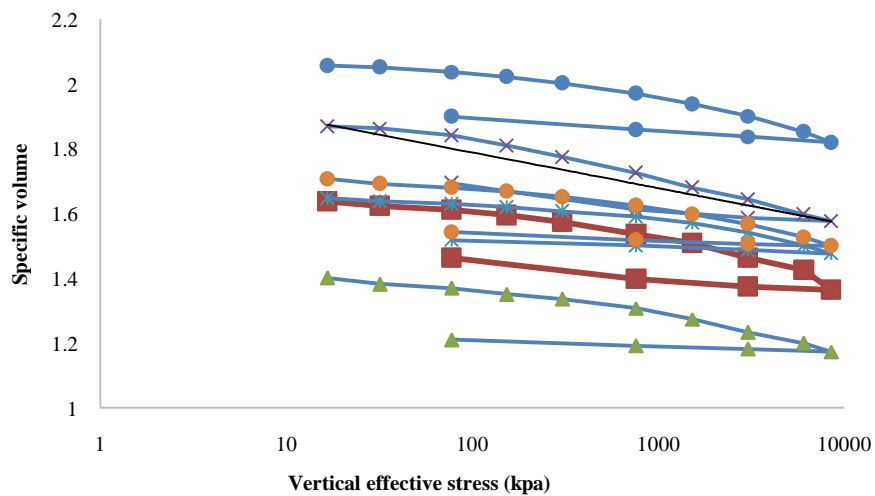


Figure 7: Compression Behavior of Samples BS

#### 4. Conclusion

One-dimensional compression tests were carried out to investigate the compression behavior of iron tailings obtained from Itakpe, Kogi state Nigeria. The samples were obtained at different depths from the tailing impoundment. The following conclusions were drawn;

1. The one-dimensional compression curves show that the paths to each sample are fairly similar and can be identified for all the tests.
2. Different sample preparation methods give fairly similar curves, so it can be considered that the behavior of the tailing materials is not significantly affected by the sample preparation methods.
3. The rates of convergence of compression curves are quite slow and transitional behavior is observed.

#### REFERENCES

- Bonin M. D, Nuth M, Dagenais A. M, and Cabral A. R. (2014). Experimental study and numerical reproduction of self-weight consolidation behavior of thickened tailings. *Journal of Geotechnical and Geo-environmental Engineering* [http://dx.doi.org/10.1061/\(ASCE\)GT.1943-5606.0001179](http://dx.doi.org/10.1061/(ASCE)GT.1943-5606.0001179)
- Blanco J. A; Vallina B; Brown A. P; and Benning L. G. (2014) Enhanced magnetic coercivity of  $\alpha$ -Fe<sub>2</sub>O<sub>3</sub> obtained from carbonated 2-line ferrihydrite. *Journal of Nanoparticle Research*. 16 (3): 2322
- Chao Z, Qinglin C, Zhenkai P and Changkun M (2019). Mechanical behavior and particle breakage of tailings under high confining pressure. *Engineering geology* 265, pp 105-419  
[doi: 10.1016/j.enggeo.2019.105419](https://doi.org/10.1016/j.enggeo.2019.105419)
- Dyvik R, Lacasse S. and Martin R. (1985) Coefficient of lateral stress from oedometer cell. *11th International Conference on Soil Mechanics and Foundation Engineering, San Francisco. 1985. Vol.2, pp. 1003-1006.*
- Ferenczi, P. (2001) Iron ore, manganese and bauxite deposits of the northern Territory. Northern Territory Geological Survey, Report 13, December 2001. pp. 13-41.
- Franks D.M, Boger D.V, Côte C.M and Mulligan D.R. (2011). Sustainable development Principles for the Disposal of Mining and Mineral Processing Wastes. *Resources Policy. Vol. 36. pp 114-122*  
<https://doi.org/10.1016/j.resourpol.2010.12.001>
- Geremew A. M & Yanful E. K. (2013). Dynamic properties and influence of clay mineralogy types on the cyclic strength of mines tailings. *International Journal of Geomechanics*  
[http://dx.doi.org/10.1061/\(ASCE\)GM.1943-5622.0000227](http://dx.doi.org/10.1061/(ASCE)GM.1943-5622.0000227)
- Hirose, K., Tateno, S. (2010). The Structure of Iron in Earth's Inner core. American Association for the Advancement of Science. pp 359-361.
- James M, Aubertin M, Wijewickreme D and Ward Wilson G. (2011). A laboratory investigation of the dynamic properties of tailings. *Journal of Geotechnical Engineering*  
<http://dx.doi.org/10.1139/t11-060>
- Li W. & Coop M.R. (2018). Mechanical behavior of Panzhihua iron tailings. *Canadian Journal of Geotechnical Engineering* 56, pp 1-16  
<https://doi.org/10.1139/cgj-2018-0032>
- McLeod H. and Bjelkevick A. (2017) History of tailing dam design. *85<sup>th</sup> annual meeting on international commission of large dams. July 3, 2017*  
<http://www.tailings.info/basics/history.htm>
- Michael W, Rahaman M.A, and Ajibade A.C. (2010). Some Metallogenetic Feature of Nigeria Basement. *Journal of African Earth Sciences* 1983. pp 655.
- Okewale IA (2019a) Influence of fines on the compression behavior of decomposed volcanic rocks. *International Journal of Geotechnical Engineering* 10(4):1-17.  
<https://doi.org/10.1186/s40703-019-0101-y>
- Okewale, I.A (2019b) Effects of weathering on the stiffness characteristics and the small strain behavior of decomposed volcanic rocks. *Journal Geological Engineering* 14(2):97-107.
- Okewale IA (2019c) On the intrinsic behavior of decomposed volcanic rocks. *Bull Eng Geol Environ*.  
<https://doi.org/10.1007/s10064-019-01643-7>
- Okewale I.A (2020) Compressibility and the Effects of Structure of Tropical Clay in Incremental Loading Oedometer Tests. *Geotech Geol Eng* (2020) 38:5355-5371  
<https://doi.org/10.1007/s10706-020-01369-4>
- Okewale IA & Coop MR (2017) A study of the effects of weathering on soils derived from decomposed volcanic rocks. *Eng Geol* 222:53-71.  
<https://doi.org/10.1016/j.enggeo.2017.03.014>
- Okewale IA & Coop MR (2020) A study of completely decomposed volcanic rocks with transitional mode of behavior. *Bull Eng Geol Environ*.  
<https://doi.org/10.1007/s10064-020-01820-z>
- Okewale IA & Grobler H (2020) A study of dynamic shear modulus and breakage of decomposed volcanic soils. *Journal of Geological Engineering* 15(1):53-66.  
[https://doi.org/10.6310/jog.202003\\_15\(1\).5](https://doi.org/10.6310/jog.202003_15(1).5)
- Okewale IA (2020) Applicability of chemical indices to characterize weathering degrees in decomposed volcanic rocks. *CATENA* 189:1-13.  
<https://doi.org/10.1016/j.catena.2020.104475>
- Okewale IA & Coop MR (2018a) On the effects of weathering on the compression behavior of decomposed volcanic rocks. *TuniRock 2018, Hammamet, Tunisia*, pp 85-90

- Okewale IA & Coop MR (2018b) Suitability of different approaches for analyzing and predicting the behavior of decomposed volcanic rocks. *Journal of Geotechnical and Geo-environmental Engineering* 144(01048064s):1–14.  
[https://doi.org/10.1061/\(ASCE\)GT.1943-5606.0001944](https://doi.org/10.1061/(ASCE)GT.1943-5606.0001944)
- Okewale IA & Coop MR (2020) A study of completely decomposed volcanic rocks with Transitional mode of behavior. *Bull Eng Geol Env.*  
<https://doi.org/10.1007/s10064-020-01820-z>
- Okewale IA & Grobler H (2020) A study of dynamic shear modulus and breakage of decomposed volcanic soils. *Journal of Geological Engineering* 15(1):53–66.  
[https://doi.org/10.6310/jog.202003.15\(1\).5](https://doi.org/10.6310/jog.202003.15(1).5)
- OlaOlorun O & Oyinloye A (2010) Geology and geotechnical appraisal of some clay deposits around Ijoro Ekiti South western Nigeria: implication for industrial uses. *Journal of Science & Indian Resources* 53(3):127–135
- Ponzoni E, Nocilla A & Coop MR (2017) The behavior of a gap graded sand with mixed Soils. *Found 57:1030–1044*.  
<https://doi.org/10.1016/j.sandf.2017.08.029>
- Rico M., Benito G., Salgueiro A. R., Díez-Herrero A., & Pereira H. G., (2008) Reported tailings dam failures. *Journal of Hazardous Materials*, vol. 152, no. 2, pp. 846–852
- Rocchi I, Coop MR & Maccarini M (2017) The effects of weathering on the physical and Mechanical properties of igneous and metamorphic saprolites. *Engineering Geology* 231:56–67  
<https://doi.org/10.1016/j.enggeo.2017.10.003>
- Rocchi I, Okewale IA & Coop MR (2015) The behavior of Hong Kong volcanic saprolites in one dimensional compression. *Balkema, Rotterdam*, pp 281–287
- Rocchi I, Coop MR & Maccarini M (2017) The effects of weathering on the physical and mechanical properties of igneous and metamorphic saprolites. *Engineering Geology* 231:56–67.  
<https://doi.org/10.1016/j.enggeo.2017.10.003>
- Rocchi I, Okewale IA & Coop MR (2015) The behavior of Hong Kong volcanic saprolites in one dimensional compression. In: *Volcanic rocks and soils. Balkema, Rotterdam*, pp 281–287
- Souza L, Tanvi P.C and Grishma S.P (2019) Case study and forensic investigation of failure of dams above kedarnath. *International society of soil mechanics and geotechnical engineering*.  
<https://www.issmge.org/publications/online-library>
- Vick S.G (1983). Planning, Design and Analysis of Tailings Dams. *John Wiley and Sons, New York*, pp. 369, ISBN 0-471-89829-5  
<https://th.bing.com/th/id/R1e53c7d3b6afc53440ab69d70f6d451a?rik=nlvKdOBCbNHfXA&pid=ImgRaw>
- Wells M, Ramanaidou E, Lau I & Laukamp C (2015). Iron ore mineralogy, processing and environmental sustainability. *Journal of Engineering geology* 298, pp 191-228.  
<https://www.researchgate.net/publication/298645505>
- Wong R, Mills B. N & Liu Y. B. (2008). Mechanistic model for one-dimensional consolidation behavior of non-segregating oil sands tailings. *Journal of Geotechnical and Geo-environmental Engineering* 134, pp 195-202  
[http://dx.doi.org/10.1061/\(ASCE\)1090-0241\(2008\)134:2\(195\)](http://dx.doi.org/10.1061/(ASCE)1090-0241(2008)134:2(195))
- Zhang L, Qi, Q, Xiong B. & Zhang J. (2011) Numerical simulation of 3-D seepage field in tailing pond and its practical application. *Procedia Engineering*, vol. 12, pp. 170–176
- Zhang L. (2013) Summary on the dam-break of tailing pond. *Journal of Hydraulic Engineering (China)*, vol. 44, no. 5, pp. 594–600